crystals

MDPI

Article

Tin Disulfide-Coated Microfiber for Humidity Sensing with Fast Response and High Sensitivity

Aijie Liang [1,†], Jingyuan Ming [1,†], Wenguo Zhu [1,*], Heyuan Guan [1], Xinyang Han [1], Shuo Zhang [1], Yuxin Lin [1], Jiangli Dong [1], Yaoming Huang [1], Wentao Qiu [1], Huihui Lu [1], Huadan Zheng [1], Yi Zhang [2,3], Jianhui Yu [1], Zhe Chen [1,*] and Ganding Peng [4]

1 Key Laboratory of Optoelectronic Information and Sensing Technologies of Guangdong Higher Education Institutes, Jinan University, Guangzhou 510632, China; aj1666274545@gmail.com (A.L.); mingjingyuan@outlook.com (J.M.); ttguanheyuan@jnu.edu.cn (H.G.); hanxinyang123@foxmail.com (X.H.); bowenpz2012@gmail.com (S.Z.); linyx@chinatelecom.cn (Y.L.); jldong@jnu.edu.cn (J.D.); yaominghuang@zjsaisi.com (Y.H.); qiuwentao@jnu.edu.cn (W.Q.); thuihuilu@jnu.edu.cn (H.L.); zhenghuadan@jnu.edu.cn (H.Z.); jianhuiyu@jnu.edu.cn (J.Y.)

2 Guangdong Engineering Technology Research Centre for High-performance Organic and Polymer Photoelectric Functional Films, Guangzhou 510275, China; ceszy@mail.sysu.edu.cn

3 State Key Laboratory of Optoelectronic Materials and Technologies, School of Chemistry, Sun Yat-Sen University, Guangzhou 510275, China

4 School of Electrical Engineering & Telecommunications, University of New South Wales, Sydney, NSW 2052, Australia; g.peng@unsw.edu.au

* Correspondence: zhuwg88@jnu.edu.cn (W.Z.); tthzhchen@jnu.edu.cn (Z.C.)

† These authors contributed equally to this work.

check for updates

Citation: Liang, A.; Ming, J.; Zhu, W.; Guan, H.; Han, X.; Zhang, S.; Lin, Y.; Dong, J.; Huang, Y.; Qiu, W.; et al. Tin Disulfide-Coated Microfiber for Humidity Sensing with Fast Response and High Sensitivity. *Crystals* **2021**, *11*, 648. https://doi.org/10.3390/cryst11060648

Academic Editors: Daquan Yang, Fei Xu and Jin-hui Chen

Received: 28 April 2021
Accepted: 24 May 2021
Published: 8 June 2021

Abstract: Breath monitoring is significant in assessing human body conditions, such as cardiac and pulmonary symptoms. Optical fiber-based sensors have attracted much attention since they are immune to electromagnetic radiation, thus are safe for patients. Here, a microfiber (MF) humidity sensor is fabricated by coating tin disulfide (SnS_2) nanosheets onto the surface of MF. The small diameter (~8 μm) and the long length (~5 mm) of the MF promise strong interaction between guiding light and SnS_2. Thus, a small variation in the relative humidity (RH) will lead to a large change in optical transmitted power. A high RH sensitivity of 0.57 dB/%RH is therefore achieved. The response and recovery times are estimated to be 0.08 and 0.28 s, respectively. The high sensitivity and fast response speed enable our SnS_2-MF sensor to monitor human breath in real time.

Keywords: two dimensional material; SnS_2; humidity sensing; microfiber

1. Introduction

Relative humidity (RH) measurement and monitoring are important for industry, food storage, human comfort, etc. [1–3]. In recent decades, various optical fiber devices have been developed for this purpose [1]. The optical fiber sensors show advantages over electronic ones, owing to their long lifetime, corrosion-free, light-weight, electromagnetic immunity, and remote sensing ability [4,5]. Microfiber and side-polished optical fiber are two kinds of optical fibers used frequently in the RH sensing [1]. To enhance the RH sensing performance, certain sensitive materials are deposited on the surface of microfiber/side-polished fiber [6,7]. In 2000, agarose gel was coated on a tapered fiber by Baríain et al. [8]. A transmitted optical power variation of 6.5 dB was obtained with a relative RH changing between 30% and 80% [8]. Recently, two dimensional (2D) materials have attracted increasing attention [9–11]. Luo et al. demonstrated an all-fiber-optic RH sensor comprised of a Tungsten disulfide (WS_2) film overlaid on a side polished fiber [11]. This sensor has a linear correlation coefficient of 99.39% [10]. Lately, Huang et al. demonstrated a high-sensitivity (0.145 nm/RH%) RH sensor by taking advantage of the swelling effect of graphene oxide film [12]. Du et al. fabricated a MoS_2-based all-fiber RH sensor with fast

response and recovery [13]. Monitoring human breath is significant for assessing human body conditions, such as cardiac and pulmonary symptoms [14,15]. Many fiber-optical RH sensors have been successfully used for monitoring human breathing [12,13]. However, ultrafast response and recovery times are required in some RH sensing application. As illustrated by [15], the infant pulmonary function testing requires a sampling rate of more than 200 Hz, which is still challenging for fiber-optical RH sensors.

Layered transition metal dichalcogenides (TMDs) have attracted much attention recently [16,17]. Compared with MoS_2 and WS_2, Tin disulfide (SnS_2) has a larger bandgap of 2.18–2.44 eV and a higher carrier mobility of ~50 $cm^2 \cdot V^{-1} \cdot s^{-1}$ [18], which guarantee its potential applications in field effect transistors [19], fast photodetectors [20], lithium-ion batteries [21,22], and visible light sensitive photo-catalyst [23]. SnS_2 has been widely used in gas-sensing [24–26]. It was demonstrated that SnS_2 nanostructures exhibit a good response and reversibility to some organic gases, such as ethanol and n-butanol [25]. Moreover, the 2D SnS_2 was shown to have a selective and reversible response for nitrogen dioxide (NO_2) with a detection limit down to 30 ppb [26]. In 2016, Bharatula fabricated an electric RH sensor based on SnS_2 [27]. However, the optical RH sensing property of SnS_2 has still not been exploited.

Here, a high-performance RH sensor is fabricated by coating SnS_2 nanosheets onto the surface of MF. The RH sensor based on SnS_2 is demonstrated to have a high RH sensitivity of 0.57 dB/%, and fast response and recovery times of 0.08 s and 0.28 s, respectively.

2. Materials and Methods

The SnS_2 suspension is purchased from Mukenano co., and is made by liquid phase exfoliation method [28]. The Raman spectrum of the SnS_2 film is excited by a 488 nm laser and measured by LabRAM HR Evolution (HORIBA JY, France) at room temperature. The measured result is shown in Figure 1a. The peak at 314 cm^{-1} is the characteristic peak of SnS_2 [18]. Figure 1b shows the absorption spectra measured by UV–visible spectroscopy. There are two main peaks of 213 nm and 256 nm in the absorption spectra, as illustrated in [29]. The absorption decreases gradually when the wavelength increases from 252 nm to 600 nm.

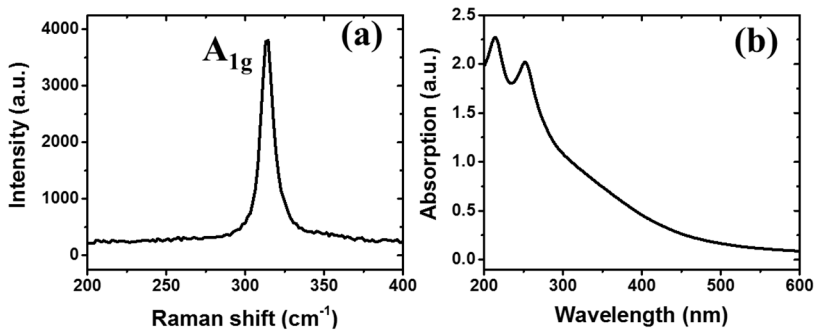

Figure 1. Raman (**a**) and UV–visible absorption spectra (**b**) of SnS_2.

The MF shown in Figure 2a is manufactured with "flame-brushing" technique [30] from a single-mode fiber (Corning SMF-28e), and has a core diameter of 8.2 μm and a cladding diameter of 125 μm. With a drawing speed of 0.2 mm/s, a MF with a diameter of ~8.18 μm in the uniform waist region is fabricated, as shown in Figure 2b, where an image of the central MF region by optical microscope is given. The dimeter changing along the MF is obtained by a series of microscopy images captured when moving the MF step by step, and the result is shown by Figure 2c. The length of uniform waist region is measured to be ~5 mm. The MF is then fixed on a glass slide by ultraviolet curing adhesive (Loctite 352, Henkel Loctite Asia Pacific). In addition, a basin (15 mm × 5 mm × 1 mm) is constituted by using the UV adhesive to contain SnS_2 solution.

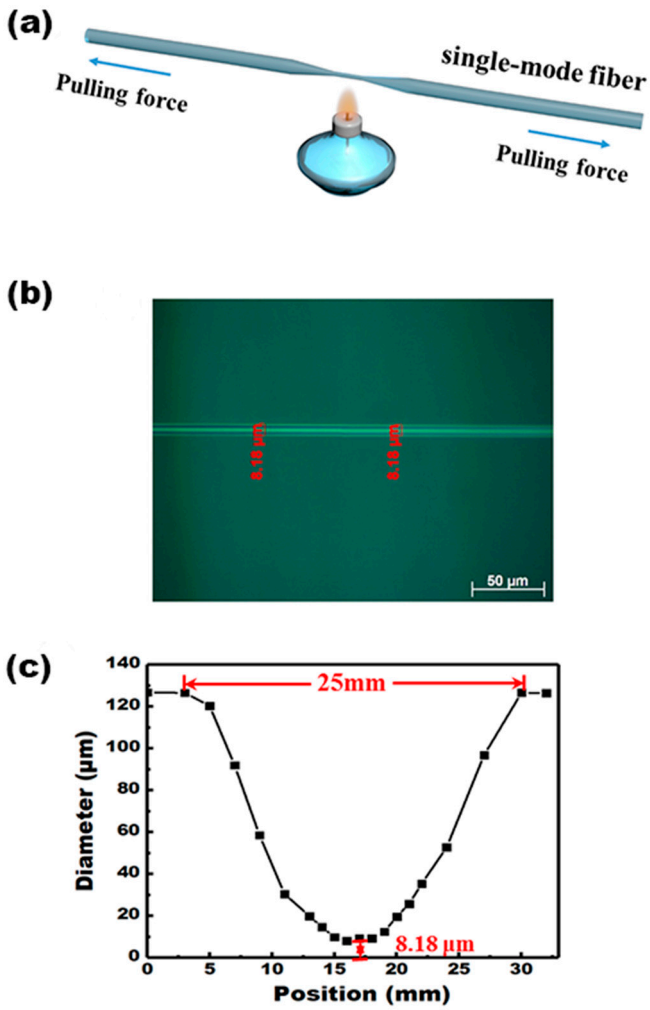

Figure 2. (**a**) Schematic of the fabrication of MF with "flame-brushing" technique. (**b**) The microscopy image of central MF region. (**c**) Morphological characteristic of MF by an optical microscopy.

For the RH sensing, we combine a MF with SnS_2 nanosheets. This is because the controllable diameter of MF can result in the strong interaction between light field and SnS_2 nanosheets. In addition, the large specific surface area of SnS_2 nanosheets enhances the absorption of water molecules. The method of depositing SnS_2 nanosheets on the MF is based on a self-assembly method. The concentration of SnS_2 alcohol suspension is 1 mg/mL. To avoid agglomeration, the SnS_2 suspension is treated by ultrasonication for 60 min. The MF is fixed in a basin, as shown by Figure 2a. As shown by Figure 3a, a 1550 nm distributed feedback (DFB) laser is launched into the MF, and the optical transmitted power is monitored. The SnS_2 alcohol suspension is dropped into the basin and evaporated naturally in ambient surrounding. During the alcohol evaporation, the SnS_2 nanosheets are self-assembling onto the MF owing to the physisorption effect, which results in the change of transmitted power, as shown by Figure 3b. After ~115 min, the power is stable at −35 dBm, indicating the complement of the self-assembly process. Recently, Zhong et al. have developed a suspended self-assembling process [31], which can improve the RH response time.

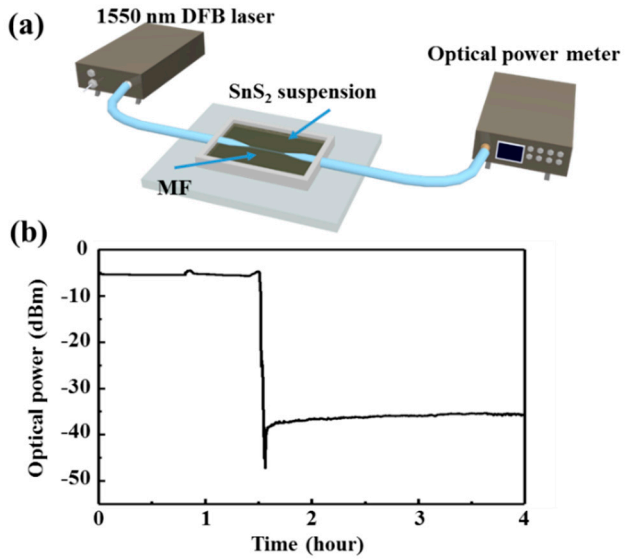

Figure 3. (**a**) Schematic setup of the deposition of SnS_2 on MF. (**b**) Variation of transmitted optical power in MF during the deposition of SnS_2 nanosheets onto the MF.

The fabricated MF coated with SnS_2 is imaged by scanning electron microscopy (SEM). As shown in Figure 4a, SnS_2 is distributed non-uniformly on the MF. The diameter of MF is 8.18 µm. The enlarged image of the SnS_2 nanosheets on MF are shown by Figure 4b, where the morphologic of SnS_2-nanosheets are shown clearly, indicating the roughness of the SnS_2 layer is about 200 nm. Figure 4c shows the SEM image of the cross section of MF, from which the thickness of the SnS_2 film is estimated to be ~161 nm.

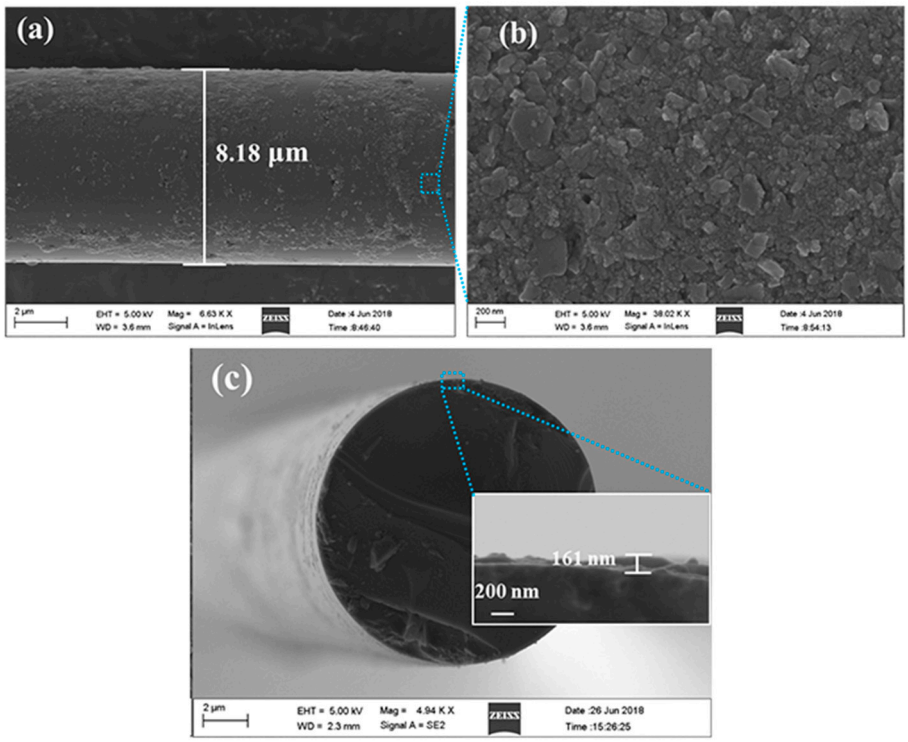

Figure 4. (**a**) SEM image of the MF coated with SnS_2. (**b**) Enlarged image of the SnS_2 nanosheets on MF. (**c**) SEM image of the cross section of MF coated with SnS_2. The inset enlarges the region marked by a dotted square.

3. Results

The RH sensing schematic is shown in Figure 5. A light from 1550 nm DFB laser source (SOF-155-D DFB LASER) is sent into MF coated with SnS_2, which is placed in a temperature-humidity chamber (BPS-100CL). The MF transmitted light is measured by optical power meter. The RH in the chamber is monitored by a commercial humidity sensor (Testo 175H1) in real time. During the RH sensing experiments, the chamber temperature is fixed at 27 °C, while the RH in the chamber ranges from ~55 %RH to ~100 %RH. Both the optical transmitted power and the RH were recorded during the whole experimental process.

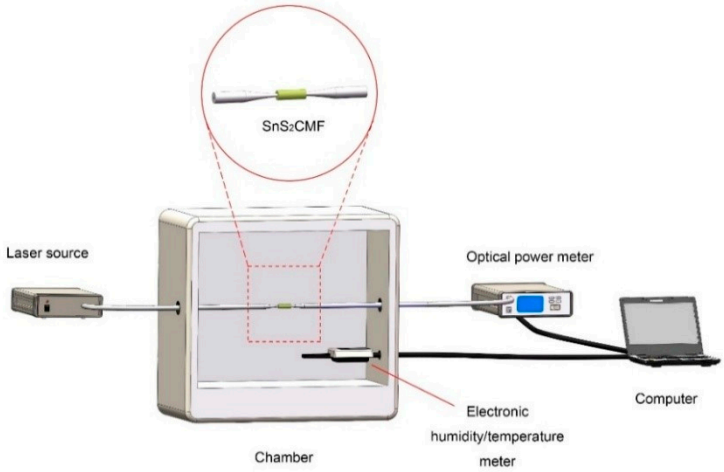

Figure 5. Experimental setup of the SnS_2-coated MF device for humidity sensing.

To test the RH sensing property, the RH in the chamber is increased and then decreased with by a step of 13 %RH in the RH range of 55% to 95%. With the change of the chamber RH, the transmitted optical power of MF coated with SnS_2 varies accordingly, as shown by Figure 6a. The variation is ~22.5 dB, ranging from ~−35 dBm to ~−13 dBm. The relationship between the transmitted power and the humidity is depicted in Figure 6b. The transmitted power in humidity ascending and descending processes are well overlapped. The transmitted power changes linearly with the chamber humidity. The sensitivity is ~0.57 dB/%RH with the R-square of ~0.98. The high sensitivity and good linearity of the SnS_2 nanosheets is appealing in the humidity sensing.

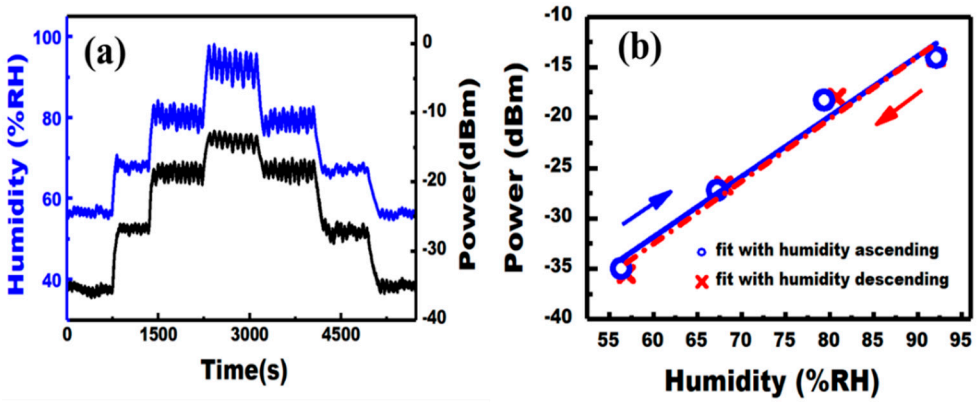

Figure 6. (**a**) Variation of the optical transmitted power with the chamber RH. (**b**) Relationship between the transmitted power and RH of SnS_2-based device.

Figure 7 shows the repeatability of the RH sensing of SnS_2-based sensor, where the chamber was switched between two RH of 45% and 100%. From the three cycles of the RH switching in Figure 7, one finds that the optical transmitted power holds the same variation

as the RH, which confirms the good repeatability and reversibility of the SnS_2-based RH sensor.

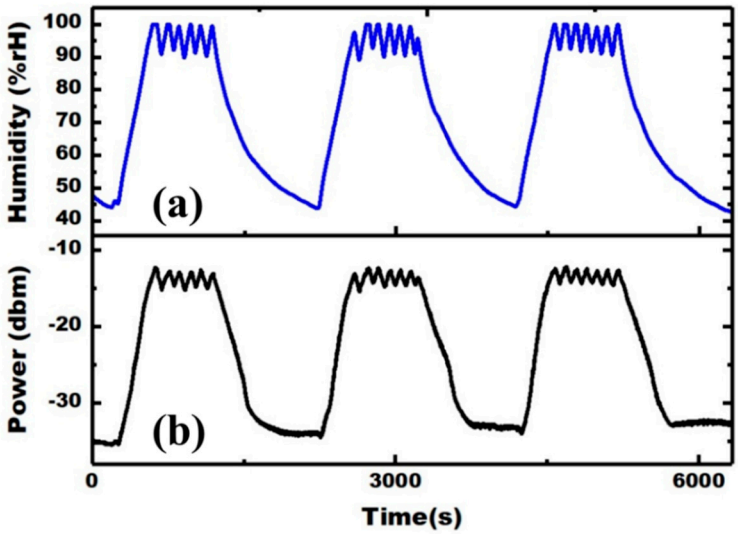

Figure 7. (**a**) Variation of RH in the chamber. (**b**) Variation of the transmitted power through the MF coated with SnS_2.

The transmitted spectrum responses of SnS_2-based sensor for the humidity were further investigated. A tunable laser (TLS, AQ4321D, ANDO) and an optical spectrum analyzer (OSA, AQ6370D, Yokogawa) were used in the experiment. Figure 8a,b show the variations of the transmitted spectrum (1520–1620 nm) for the RH ascending (a) and descending (b) processes, respectively. The transmitted spectrum of the MF with SnS_2 undergoes a relative change when the RH changes in the range of 50% to 95%.

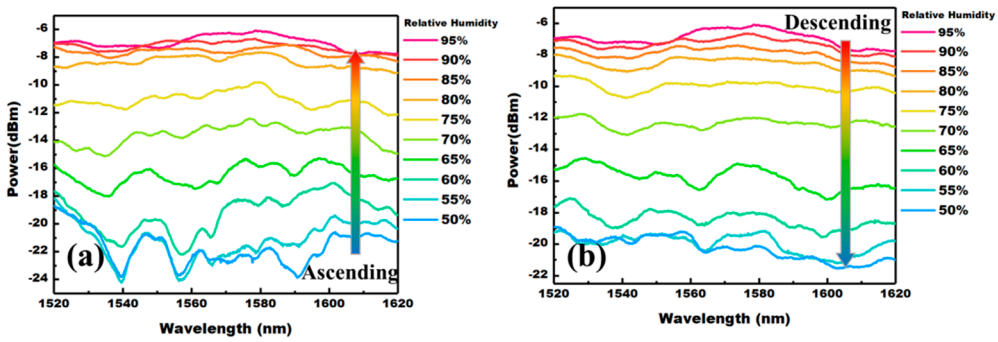

Figure 8. The variation of the transmitted spectrum in RH ascending (**a**) and descending (**b**) processes.

As shown by Figures 6 and 8, the transmitted power increases with the relative RH, which should be a result of the increase of the real part of the refractive index of SnS_2. In contrast to the RH sensor-based graphene oxide [12,31], the swelling effect of TMDs is not obvious [32]. When water molecules are absorbed by SnS_2 film, some air is replaced by the water molecules. Thus, the average refractive index should be $n = f_{SnS_2} n_{SnS_2} + f_{air} n_{air} + f_{water} n_{water}$, where n_x and f_x (x = SnS_2, air, water) are the refractive index and filling factor, respectively. As $f_{SnS_2} + f_{air} + f_{water} = 1$ and $n_{water} > n_{air}$, the absorption of water molecules increases the average refractive index.

To investigate the influence of the SnS_2 refractive index on the absorption of SnS_2-coated MF, we perform a simulation with COMSOL Multiphysics. The simulated structure is shown by Figure 9a, which is the same as the experimental one. The refractive index of MF and SnS_2 are 1.46 and 2.29 + 0.3i [33], respectively. The intensity distributions of fundamental modes with and without SnS_2 are shown by Figure 9b. The light field is

enhanced and absorbed by the SnS_2 film, as shown by Figure 9c. With the increase of the real part of the refractive index of SnS_2 film, the imaginary part of effective index of SnS_2-coated MF decreases gradually, resulting in the increase of the transmitted power as observed experimentally.

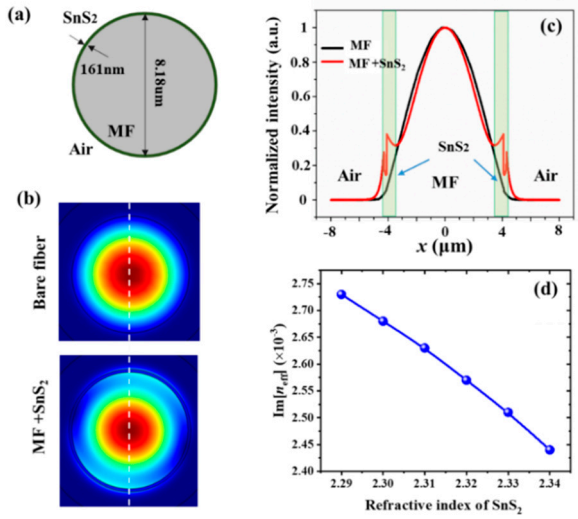

Figure 9. (**a**) The structure of the SnS_2-coated MF. (**b**) Intensity patterns of fundamental modes with and without SnS_2 film. (**c**) Normalized intensity along the dotted lines in (**b**). (**d**) Imaginary part of effective index of SnS_2-coated MF changing with refractive index of SnS_2.

It is interesting to apply the SnS_2-based MF sensor for monitoring human breath. The experimental setup to monitor human breath is shown in Figure 10a. A light from 1550 nm DFB laser is launched into SnS_2-coated MF. The transmitted optical light is detected by a photodetector (1811, New Focus), and the transformed electric signal is analyzed by an oscilloscope (DS1052E, Rigol). Figure 10b shows the five cycles of human breathing. The photodetector voltage varies in accordance with the evolution of the exhale/inhale cycles with a maximum voltage variation of ~0.2 V. According to the enlarged view of the response from the fourth cycle, the best response and recovery times are 0.08 s and 0.28 s, respectively. The average response and recovery times over five human breathing cycles are 0.10 s and 0.31 s, respectively.

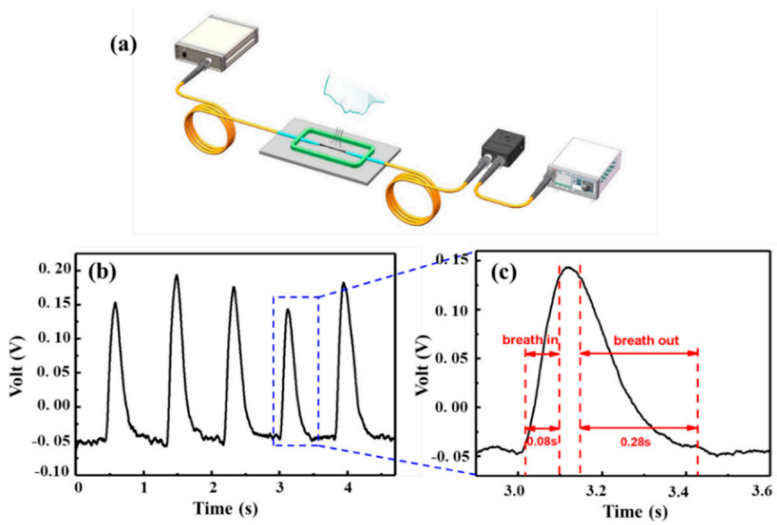

Figure 10. (**a**) Experimental setup for monitoring human breath. (**b**) Response characteristic of human breath with five cycles. (**c**) Enlarged view of the response from the fourth cycle to evaluate the response time and recovery time.

Table 1 shows the main performances of our proposed device and other types of recently developed fiber-optical humidity sensors in literature. Compared to the other fiber-optical RH sensors, the SnS_2-based MF device possesses a much higher sensitivity with a high linearity in the RH range of 55 %RH–95 %RH. Moreover, the sum of response and recovery time (total time) of our sensor is the smallest (0.36 s), which is at least more than 4.7 times smaller than other fiber RH sensors activated with layered TMDs. Compared to the MoS_2-coated etched single-mode fiber, our sensor possesses a little slower response time of 0.08 s, but a faster recovery time of 0.28 s [13]. Therefore, the SnS_2-based MF device is more suitable for the human breath monitoring.

Table 1. Comparison of the main performance between the proposed SnS_2-coated MF sensor and other recently developed fiber-optic sensing devices in the literature.

Device Structure	Response Time (s)	Recovery Time (s)	Total Time(s)	Dynamic Range of Response
MoS_2 nanosheets based SPF [9]	0.85	0.85	1.70	0.33 dB/%RH (40 %RH–85 %RH)
MoS_2-coated etched single-mode fiber [13]	0.066	2.395	2.461	0.008 dB/%RH (20 %RH–80 %RH)
$MoSe_2$-coated fiber-optic sensor [34]	1	4	5	0.26 dB/%RH (32 %RH–73 %RH)
Tungsten disulphide (WS_2)-coated	1	4	5	0.17 dB/%RH (37 %RH–90 %RH)
Graphene oxide (GO)-coated fiber-optic sensor [11]	2.73	7.27	10.0	0.427 dB/%RH (59 %RH–93 %RH)
Agarose gel with tapered fiber [7]	5	55	60	0.13 dB/%RH (30 %RH–80 %RH)
SnS_2-coated MF (this paper)	0.08	0.28	0.36	0.57 dB/%RH (55 %RH–95 %RH)

4. Conclusions

A high-performance RH sensor has been proposed by coating SnS_2 nanosheets onto the surface of an MF. Due to the strong interaction between evanescent wave of MF and SnS_2 nanosheets, the SnS_2-based sensor possesses a high sensitivity of 0.57 dB/%RH in the RH range of 55 %RH–95 %RH. The response and recovery times respectively are 0.08 s and 0.28 s, allowing us to monitor human breath in real time. This optical RH sensor may find applications in medical diagnosis.

Author Contributions: Conceptualization, A.L. and J.M.; methodology, A.L. and J.M.; software, A.L., J.M., W.Z., H.G. and X.H.; validation, A.L., J.M., W.Z., H.G., S.Z., Y.L. and Y.H.; formal analysis, S.Z., Y.L., Y.H. and W.Z.; investigation, Y.Z. and H.Z.; resources, Y.Z. and J.Y.; data curation, A.L., J.M., W.Z., H.G. and X.H.; writing—original draft preparation, A.L. and J.M.; writing—review and editing, H.G., J.D., W.Q. and H.L.; supervision, Z.C., H.L., H.G. and G.P.; project administration, Z.C., H.L., H.G. and G.P. All authors have read and agreed to the published version of the manuscript.

Funding: Please add: This research was funded by the NSAF (Grant No. U2030103); National Natural Science Foundation of China (61775084, 61705089, 61705087, 62075088,61505069); Guangdong Special Support Program(2016TQ03X962); Natural Science Foundation of Guangdong Province (2020A151501791, 2021A1515011875); Open Fund of Guangdong Provincial Key Laboratory of Information Photonics Technology of Guangdong University of Technology (No. GKPT20-03). Fundamental Research Funds for the Central Universities (11620444).

Institutional Review Board Statement: Not applicable.

Informed Consent Statement: Not applicable.

Data Availability Statement: Not applicable.

Acknowledgments: Work was supported by the Guangdong Engineering Technology Research Centre for High-performance Organic and Polymer Photoelectric Functional Films.

Conflicts of Interest: The authors declare no conflict of interest.

References

1. Ascorbe, J.; Corres, J.M.; Arregui, F.J.; Matias, I.R. Recent developments in fiber optics humidity sensors. *Sensors* **2017**, *17*, 893. [CrossRef]
2. Gomez, D.; Morgan, S.P.; Hayes-Gill, B.R.; Correia, R.G.; Korposh, S. Polymeric optical fibre sensor coated by SiO_2 nanoparticles for humidity sensing in the skin microenvironment. *Sens. Actuators B Chem.* **2018**, *254*, 887–895. [CrossRef]
3. Yang, M.; Xie, W.; Dai, Y.; Lee, D.; Dai, J.; Zhang, Y.; Zhuang, Z. Dielectric multilayer-based fiber optic sensor enabling simultaneous measurement of humidity and temperature. *Opt. Express* **2014**, *22*, 11892. [CrossRef]
4. Lou, J.; Wang, Y.; Tong, L. Microfiber optical sensors: A review. *Sensors* **2014**, *14*, 5823–5844. [CrossRef]
5. Chen, J.; Xiong, Y.; Xu, F.; Lu, Y. Silica optical fiber integrated with two-dimensional materials: Towards opto-electro-mechanical technology. *Light Sci. Appl.* **2021**, 10. [CrossRef]
6. Guan, H.; Xia, K.; Chen, C.; Luo, Y.; Tang, J.; Lu, H.; Yu, J.; Zhang, J.; Zhong, Y.; Chen, Z. Tungsten disulfide wrapped on micro fiber for enhanced humidity sensing. *Opt. Mater. Express* **2017**, *7*, 1686. [CrossRef]
7. Ascorbe, J.; Corres, J.M.; Matias, I.R.; Arregui, F.J. High sensitivity humidity sensor based on cladding-etched optical fiber and lossy mode resonances. *Sens. Actuators B Chem.* **2016**, *233*, 7–16. [CrossRef]
8. Bariáin, C.; Matías, I.R.; Arregui, F.J.; López-Amo, M. Optical fiber humidity sensor based on a tapered fiber coated with agarose gel. *Sens. Actuators B Chem.* **2000**, *69*, 127–131. [CrossRef]
9. Li, D.; Lu, H.; Qiu, W.; Dong, J.; Guan, H.; Zhu, W.; Yu, J.; Luo, Y.; Zhang, J.; Chen, Z. Molybdenum disulfide nanosheets deposited on polished optical fiber for humidity sensing and human breath monitoring. *Opt. Express* **2017**, *25*, 28407. [CrossRef]
10. Wang, Y.; Shen, C.; Lou, W.; Shentu, F.; Zhong, C.; Dong, X.; Tong, L. Fiber optic relative humidity sensor based on the tilted fiber Bragg grating coated with graphene oxide. *Appl. Phys. Lett.* **2016**, *109*, 1–6. [CrossRef]
11. Luo, Y.; Chen, C.; Xia, K.; Peng, S.; Guan, H.; Tang, J.; Lu, H.; Yu, J.; Zhang, J.; Xiao, Y.; et al. Tungsten disulfide (WS_2) based all-fiber-optic humidity sensor. *Opt. Express* **2016**, *24*, 8956. [CrossRef]
12. Huang, Y.; Zhu, W.; Li, Z.; Chen, G.; Chen, L.; Zhou, J.; Lin, H.; Guan, J.; Fang, W.; Liu, X.; et al. High-performance fibre-optic humidity sensor based on a side-polished fibre wavelength selectively coupled with graphene oxide film. *Sens. Actuators B Chem.* **2018**, *255*, 57–69. [CrossRef]
13. Du, B.; Yang, D.; She, X.; Yuan, Y.; Mao, D.; Jiang, Y.; Lu, F. MoS_2-based all-fiber humidity sensor for monitoring human breath with fast response and recovery. *Sens. Actuators B Chem.* **2017**, *251*, 180–184. [CrossRef]
14. Yasuma, F.; Hayano, J.I. Respiratory Sinus Arrhythmia: Why Does the Heartbeat Synchronize with Respiratory Rhythm? *Chest* **2004**, *125*, 683–690. [CrossRef]
15. Bates, J.H.T.; Schmalisch, G.; Filbrun, D.; Stocks, J. Tidal breath analysis for infant pulmonary function testing. *Eur. Respir. J.* **2000**, *16*, 1180–1192. [CrossRef] [PubMed]
16. Schaibley, J.R.; Yu, H.; Clark, G.; Rivera, P.; Ross, J.S.; Seyler, K.L.; Yao, W.; Xu, X. Valleytronics in 2D materials. *Nat. Rev. Mater.* **2016**, 1. [CrossRef]
17. Mahmood, F.; Alpichshev, Z.; Lee, Y.H.; Kong, J.; Gedik, N. Observation of Exciton-Exciton Interaction Mediated Valley Depolarization in Monolayer $MoSe_2$. *Nano Lett.* **2018**, *18*, 223–228. [CrossRef] [PubMed]
18. Ye, G.; Gong, Y.; Lei, S.; He, Y.; Li, B.; Zhang, X.; Jin, Z.; Dong, L.; Lou, J.; Vajtai, R.; et al. Synthesis of large-scale atomic-layer SnS_2 through chemical vapor deposition. *Nano Res.* **2017**, *10*, 2386–2394. [CrossRef]
19. Liu, J.; Xia, C.; Li, H.; Pan, A. High on/off ratio photosensitive field effect transistors based on few layer SnS_2. *Nanotechnology* **2016**, *27*, 1–6. [CrossRef]
20. Su, G.; Hadjiev, V.G.; Loya, P.E.; Zhang, J.; Lei, S.; Maharjan, S.; Dong, P.M.; Ajayan, P.; Lou, J.; Peng, H. Chemical vapor deposition of thin crystals of layered semiconductor SnS_2 for fast photodetection application. *Nano Lett.* **2015**, *15*, 506–513. [CrossRef]
21. Zhou, T.; Pang, W.K.; Zhang, C.; Yang, J.; Chen, Z.; Liu, H.K.; Guo, Z. Enhanced sodium-ion battery performance by structural phase transition from two-dimensional hexagonal-SnS_2 to orthorhombic-SnS. *ACS Nano* **2014**, *8*, 8323–8333. [CrossRef] [PubMed]
22. Qu, B.; Ma, C.; Ji, G.; Xu, C.; Xu, J.; Meng, Y.S.; Wang, T.; Lee, J.Y. Layered SnS_2-reduced graphene oxide composite—A high-capacity, high-rate, and long-cycle life sodium-ion battery anode material. *Adv. Mater.* **2014**, *26*, 3854–3859. [CrossRef]
23. Zhang, Y.; Zhang, F.; Yang, Z.; Xue, H.; Dionysiou, D.D. Development of a new efficient visible-light-driven photocatalyst from SnS_2 and polyvinyl chloride. *J. Catal.* **2016**, *344*, 692–700. [CrossRef]
24. Xu, K.; Li, N.; Zeng, D.; Tian, S.; Zhang, S.; Hu, D.; Xie, C. Interface bonds determined gas-sensing of SnO_2-SnS_2 hybrids to ammonia at room temperature. *ACS Appl. Mater. Interfaces* **2015**, *7*, 11359–11368. [CrossRef]
25. Huang, J.; Yu, K.; Gu, C.; Zhai, M.; Wu, Y.; Yang, M.; Liu, J. Preparation of porous flower-shaped SnO_2 nanostructures and their gas-sensing property. *Sens. Actuators B Chem.* **2010**, *147*, 467–474. [CrossRef]
26. Ou, J.Z.; Ge, W.; Carey, B.; Daeneke, T.; Rotbart, A.; Shan, W.; Wang, Y.; Fu, Z.; Chrimes, A.F.; Wlodarski, W.; et al. Physisorption-Based Charge Transfer in Two-Dimensional SnS_2 for Selective and Reversible NO_2 Gas Sensing. *ACS Nano* **2015**, *9*, 10313–10323. [CrossRef] [PubMed]
27. Bharatula, L.D.; Erande, M.B.; Mulla, I.S.; Rout, C.S.; Late, D.J. SnS_2 nanoflakes for efficient humidity and alcohol sensing at room temperature. *RSC Adv.* **2016**, *6*, 105421–105427. [CrossRef]
28. Fu, X.; Ilanchezhiyan, P.; Mohan Kumar, G.; Cho, H.D.; Zhang, L.; Chan, A.S.; Lee, D.J.; Panin, G.N.; Kang, T.W. Tunable UV-visible absorption of SnS_2 layered quantum dots produced by liquid phase exfoliation. *Nanoscale* **2017**, *9*, 1820–1826. [CrossRef]

29. Wang, C.; Tang, K.; Aa, Q.Y.; Qian, Y. Raman scattering, far infrared spectrum and photoluminescence of SnS_2 nanocrystallites. *Chem. Phys. Lett.* **2002**, *357*, 371–375. [CrossRef]
30. Wu, X.; Tong, L. Optical microfibers and nanofibers. *Nanophotonics* **2013**, *2*, 407–428. [CrossRef]
31. Zhong, Y.; Wang, Y.; Wang, Z.; Xing, Z.; Xiao, Y.; Yu, J.; Guan, H.; Luo, Y.; Lu, H.; Zhu, W.; et al. Ultrafast freestanding microfiber humidity sensor based on three-dimensional graphene network cladding. *Opt. Express* **2020**, *28*, 4362. [CrossRef] [PubMed]
32. Hirunpinyopas, W.; Prestat, E.; Worrall, S.D.; Haigh, S.J.; Dryfe, R.A.W.; Bissett, M.A. Desalination and Nanofiltration through Functionalized Laminar MoS_2 Membranes. *ACS Nano* **2017**, *11*, 11082–11090. [CrossRef]
33. Amroun, M.N.; Khadraoui, M.; Miloua, R.; Kebbab, Z.; Sahraoui, K. Investigation on the structural, optical and electrical properties of mixed SnS_2—CdS thin films. *Optik* **2017**, *131*, 152–164. [CrossRef]
34. Lang, Y.; Ouyang, T.; Lin, L.; Xia, K.; Jiang, M.; Guan, H.; Yu, J.; Li, D.; Chen, G.; Zhu, W.; et al. Side polished fiber coated with molybdenum diselenide ($MoSe_2$) for humidity sensing. *Sensors* **2017**, *25*, SeW1E.2. [CrossRef]